Int. J. Heat Mass Transfer. Vol. 35, No. 12, pp. 3353–3362, 1992
Printed in Great Britain

0017–9310/92 $5.00+0.00

Experimental methods of estimating heat transfer in circulating fluidized bed boilers

BENGT-ÅKE ANDERSSON and BO LECKNER
Department of Energy Conversion, Chalmers University of Technology, S-412 96 Göteborg, Sweden

(*Received* 22 *July* 1991 *and in final form* 27 *November* 1991)

Abstract—Four different experimental methods have been used for the estimation of the bed-to-membrane wall heat transfer in a 12 MW_{th} circulating fluidized bed boiler. The methods are compared for a case of normal operating conditions and the measured heat transfer coefficients are presented. In the central part of the combustion chamber where most of the cooling surface is located, the cross-sectional average suspension density normally varies in the range of 10–20 kg m^{-3} and the heat transfer coefficient is around 130 W m^{-2} K^{-1} with a scatter of ±15% due to the different methods. The methods are critically analyzed and the heat transfer data are compared with relevant literature data.

INTRODUCTION

VERY little information about heat transfer in circulating fluidized bed boilers (CFBB) is available [1]. One reason is of course, that this technology has only recently been applied in commercial scale applications where realistic measurements are possible. Another reason for the scarce information is the inaccessibility of the boiler combustion chambers. The flow of particles at the walls may cause severe erosion, and all kinds of unevenness such as apertures required for inserting measurement probes, are carefully avoided in commercial boilers. Therefore, the combustion chambers are generally not accessible for measurements.

At Chalmers University of Technology a research boiler has been built. Due to special design features (hot-water boiler) and to the fact that this is a research installation, holes for probes are available in the walls. This makes various kinds of measurements possible. Below, methods of heat transfer measurements will be investigated, using probes as well as the boiler walls themselves. The purpose of the work is to compare such methods.

EXPERIMENTS

The Chalmers CFBB has a capacity of 12 MW thermal power at full load. The combustion chamber, consisting of membrane tube walls, has a cross-section of 1.7 m by 1.7 m and is 13.5 m tall. The bottom part, from 0 to 2 m height, is covered with a 0.11 m thick layer of refractory to prevent tube erosion. In addition, two of the walls are refractory lined in order to maintain the desired suspension temperature throughout the combustion chamber.

Two types of membrane wall are common [2]; the 'American type' where the fin is welded to the tube and the 'Walther type' where the fin is a part of the tube. The latter type is used in the present boiler, as shown in Fig. 1. The outer tube diameter is 60.3 mm, tube wall thickness 5.6 mm, fin length 8.8 mm, fin thickness 6.0 mm and the radius of the fin-tube junction is 4.0 mm. In two symmetric locations on the opposite cold walls, two of the fins are prolonged to 12.4 mm resulting in a tube pitch of 85 mm.

The cold walls contain a large number of thermocouples for heat flow measurements recording the local fin and tube temperature in positions 7 and 10 in Fig. 1. Such pairs of thermocouples (positions 7 and 10) are mounted on eight tubes, numbers 1 to 6 on one wall and numbers 7 and 8 on the opposite wall, see Fig. 2. In one location, on tube number 5 at 7 m height, the temperature is measured in all ten positions shown in Fig. 1. Near the hot junction, each thermocouple was vertically mounted along the tube, i.e. isothermally, for a distance of about 50 mm to prevent an error due to heat conduction in the thermocouple itself. On the bed side, the thermocouples were placed 1 mm below the tube surface and covered by silver sold in order to protect them from erosion. The accuracy of the thermocouples is ±0.06%, i.e. ±0.12 K at a temperature of 200°C.

The walls are also provided with 50 mm diameter holes through which various meters can be introduced, Fig. 2. The cross-section of such a hole is shown in Fig. 3.

Primary air is supplied through the distributor plate in the bottom of the combustion chamber, as shown in Fig. 2, and secondary air may be introduced at several heights from nozzles in the two opposite refractory lined walls. The fuel is fed through a chute in the front wall.

The comparison between different methods of heat transfer measurements will be made for one test run during which the boiler was operated at steady state conditions for more than five hours with the bulk bed temperature 850°C, the fluidization velocity 6.3 m s^{-1}

NOMENCLATURE

A_{cw}	total surface area of cold walls [m^2]	p	pressure [Pa]
A_i	surface area of ith cold wall element [m^2]	$\dot{q}_i$	heat flow at ith wall element [W m^{-2}]
C_1	constant in equation (2) [Pa]	$\dot{Q}_{cw}$	total heat power to cold walls [W]
C_2	constant in equation (3) [kg m^{-1} s^{-2}]	T_{bed}	bed temperature [°C]
C_3	constant in equation (6) [W m^{-2} K^{-1}]	T_{fin}	fin temperature [°C]
C_4	constant in equation (8) [kg$^{1/2}$ m$^{3/2}$ s^{-3} K^{-1}]	T_{tube}	tube surface temperature [°C]
$\bar{d}$	mean particle diameter [m]	x_i	mass fraction of ith particle diameter [−].
d_i	particle diameter of ith mass fraction [m]		
F, F_i	correction factor in equation (6) [−]		
g	gravitational acceleration constant [m s^{-2}]	Greek symbols	
h	height [m]	α	heat transfer coefficient [W m^{-2} K^{-1}]
		ρ	suspension density [kg m^{-3}].

and 30% of the air supplied as secondary air at a height of 2.2 m above the bottom of the bed. These conditions are typical for normal operation of the boiler.

The average bulk bed temperature is evaluated from temperatures measured in three positions in the bottom of the bed and in three positions in the top. In the present case, the temperature difference between the various measurement positions was less than 10 K. Hence, the variation is small and a fairly good estimate of the average temperature of the bulk of the bed is achieved.

The bed material was silica sand with a particle density of 2600 kg m^{-3} and the fuel was bituminous coal 0–20 mm in size. The particle size distributions of the sand, the bed and the material in the cyclone leg are given in Fig. 4. The corresponding mean particle sizes calculated from equation (1) are 324, 312 and 244 μm respectively.

$$\bar{d} = \frac{1}{\sum_i \frac{x_i}{d_i}}. \tag{1}$$

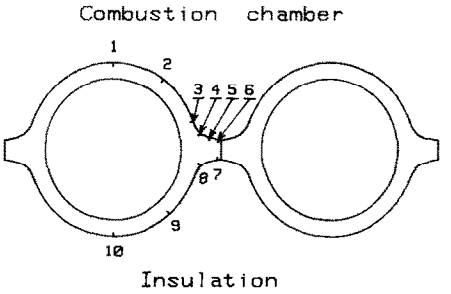

FIG. 1. Membrane wall section. Numbers 1–10 indicate thermocouple locations used in the present measurements. Numbers 7 and 10 are used for heat flow measurements. The remaining thermocouples together with 7 and 10 are used to investigate the distribution of temperature around the tube–fin geometry in order to determine the corresponding distribution of heat flow.

The axial distribution of suspension density is obtained from pressure measurements in taps located at one of the cold walls and about half a meter apart except in the bottom zone where they are more closely spaced. In order to get a smooth suspension density curve the pressure gradient was correlated by the logarithmic expression

$$p = C_1 + C_2 \ln h \tag{2}$$

with differentiation yielding the suspension density,

$$\rho = -\frac{1}{g}\frac{C_2}{h} \tag{3}$$

since

$$\rho = -\frac{1}{g}\frac{\mathrm{d}p}{\mathrm{d}h}. \tag{4}$$

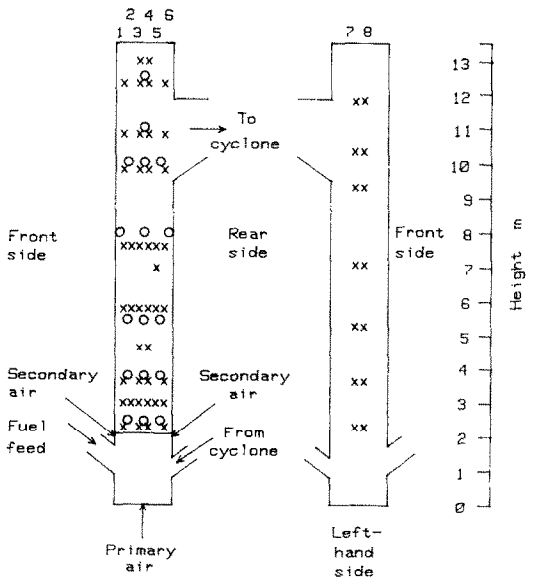

FIG. 2. The two opposite cold walls of the combustion chamber. (O) holes, (X) fin–tube thermocouples on eight tubes, numbers 1–8.

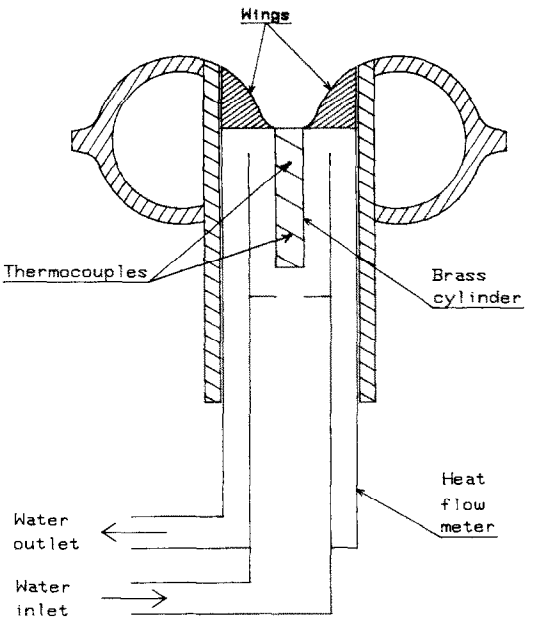

FIG. 3. Cross-section of a hole in membrane wall showing a heat flow meter in measurement position.

The constants C_1 and C_2 are obtained from a fit of equation (2) to the measured pressures. The correlation is based only on the pressures measured at the cooling surface. The suspension density in the case treated varies from 45 kg m^{-3} at 2 m height to 10 kg m^{-3} at 11 m height, as shown in Fig. 5. The total pressure drop in the combustion chamber was 5.88 kPa.

METHODS OF HEAT TRANSFER MEASUREMENTS

Method 1. *Heat balance*

An average heat transfer coefficient between the bed and the cold membrane walls can be calculated from

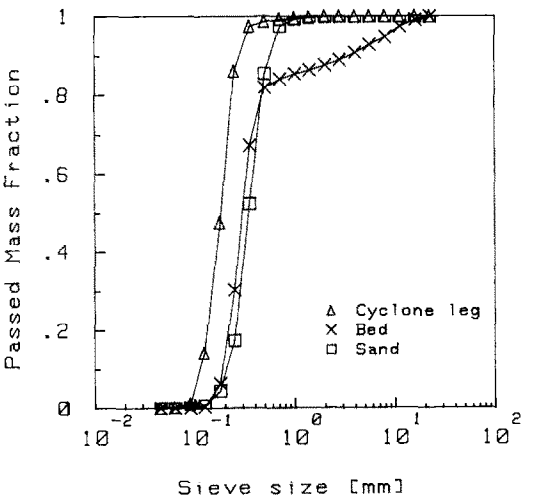

FIG. 4. Particle size distributions of the sand supplied (□), material from bed (X) and cyclone leg (△).

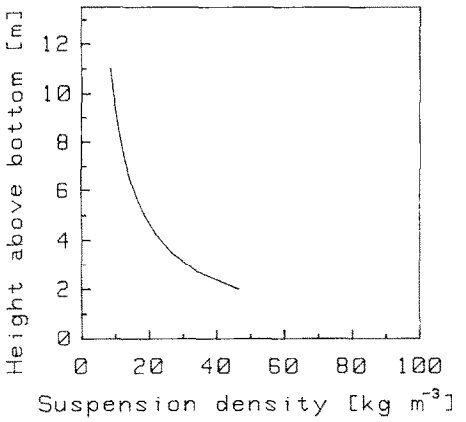

FIG. 5. Suspension density profile.

a heat balance over the combustion chamber since this part of the boiler is separated from the other parts on the water side. The average heat transfer coefficient α is obtained from the total heat power absorbed by the cold membrane tube walls $\dot{Q}_{cw}$, and the total tube and fin surface area A_{cw}. The choice of area is based on a previous analysis on heat transfer in CFBB [3]. The difference in temperature between the bulk of the bed, T_{bed}, and the crest of the tube, T_{tube}, position 1 in Fig. 1, is used in the definition of a heat transfer coefficient,

$$\alpha = \frac{\dot{Q}_{cw}}{A_{cw}(T_{bed} - T_{tube})}. \quad (5)$$

The variation in temperature around the tube and fin in a CFBB is small compared with the temperature difference between the bulk of the bed and the wall surface. Hence, the temperature of the surface at the tube crest is a satisfactory representation of the local wall temperature. The tube temperature used in equation (5) is an average value over the height of the combustion chamber, since the tube temperature increases as the cooling water is heated up.

The small amount of heat (about 10%) absorbed by the refractory lined surfaces is determined by means of pairs of thermocouples sensing the temperature gradient inside the refractory material. This quantity of heat is taken into account in the heat balance and is not included in $\dot{Q}_{cw}$. Seventeen of these pairs are located in the combustion chamber refractory which covers about 54 m^2 wall surface area corresponding to about 60% of the total projected area. The thermal conductivity of the refractory, analyzed with the Transient Hot-strip Technique [4], is given in Table 1 vs temperature.

Method 2. *Local heat flow meters*

A water cooled conductivity type of heat flow meter was inserted through the holes shown in Fig. 2 and positioned flush with the fin (Fig. 3). The meter is provided with 'wings' to cover the hole and to avoid disturbing the flow of particles along the wall. The

Table 1. Thermal conductivity of refractory material and tube steel

Material	Temperature (°C)	Thermal conductivity (W m^{-1} K^{-1})
Refractory	21	1.63
	100	1.97
	200	1.94
Steel	24	45.0
	100	50.5
	150	50.2
	200	50.6
	250	48.4
	300	46.7
	350	43.8

diameter of the meter is 48 mm. The conductivity plug is a 10 mm diameter and 50 mm long brass cylinder which yields the local value of heat flow at the fin by means of two temperatures measured in the center of the brass cylinder. The cylinder is insulated by means of two concentric guard rings surrounding the sides of the cylinder. The heat flow meter is calibrated in a black-body furnace and the accuracy is around $\pm 10\%$ [5]. The heat transfer coefficient is calculated from the measured heat flow and the difference between the temperature of the bulk of the bed and of the surface of the meter. The latter temperature is obtained from an extrapolation with the assumption of a linear temperature gradient in the brass cylinder.

Method 3. *Local water temperature*

In Method 3 the local temperature of the cooling water flowing inside the tubes is determined from the measured tube temperature in position 10 (Fig. 1), the heat conductivity of the tube steel given in Table 1, the tube wall thickness, and the inside heat transfer coefficient (around 5000 W m^{-2} K^{-1}). The last quantity is derived from a calculated average mass flow rate of water in the tubes of the cold walls and a conventional expression of heat transfer for turbulent tube flow. Local values of absorbed heat are then estimated from the increase in water temperature along a tube. The bed-to-wall heat transfer coefficient is based, also in this case, on the temperature of the bulk of the bed and of the crest of the tube.

The accuracy of this method, which recently has been used in a laboratory scale CFB measurement [6], can be low if the temperature increase is low. Moreover, it is not applicable if boiling occurs.

Method 4. *Fin–tube temperature difference*

Methods 3 and 4 are based on wall temperatures measured at locations on the walls denoted by crosses in Fig. 2 and in various positions around the tube geometry shown in Fig. 1. Method 3 relies on the temperature in position 10, whereas method 4 also uses the fin temperature in position 7.

A common method of evaluating heat absorption in boiler tubes is to analyze the temperature field in the metal [2, 7, 8, 9, 10]. The calculated and measured temperatures are compared for various positions on the tube. In the present investigation, two positions on the insulated side of the membrane wall, the fin end and the tube crest (number 7 and 10 in Fig. 1) were selected, and provided with 1 mm diameter Chromel–Alumel thermocouples. In these positions the thermocouples are easy to mount and they are not exposed to erosion. Moreover, they are located on lines of symmetry, see Fig. 1, where the temperature gradient is small, which favours the accuracy of the measurement.

Figure 2 shows the locations of the fin–tube thermocouples. It should be pointed out that the centerline tubes are instrumented with thermocouples in both cold walls, tubes numbers 3, 4, 7 and 8 in Fig. 2, in order to check the symmetry of the heat transfer in the combustion chamber. In addition, these four tubes were provided with prolonged fins to give a larger temperature difference between fin and tube and thus a higher accuracy than for tubes with normal fin length.

A considerable amount of work has been spent on the evaluation of the heat flow from the temperature measurements by calculation of the two-dimensional temperature field resulting in rather complex approximate analytical expressions [7, 10]. Also, numerical methods have been tried. If a finite difference method with rectangular cells is chosen, special considerations have to be made for the junction between fin and tube [10]. A more suitable choice is a finite element scheme which handles the mixed character of the fin–tube geometry without any problem. Therefore, a standard finite element program is employed in the present analysis. The remaining difficulty in the calculation is to apply a proper boundary condition on the bed side of the wall geometry. In work on pulverized coal or recovery boilers where radiation dominates the heat transfer, the radiant heat is assumed to be uniform away from the wall and distributed around the tube and fin according to the radiation view factors [2, 7, 8]. In a CFBB on the other hand, the situation is more complex due to the presence of particles near the wall. Visual observations and temperature measurements on the Chalmers boiler [11] indicate that the concentration of particles is higher and the temperature of the suspension is lower at the fin than at the tube crest. These variations around the tube should be considered in an analysis of the temperature field in the tube.

In the present work, the relation between the bed side heat flow and the fin–tube temperature difference at steady-state is calculated by means of the finite element program Ace [12] with the geometry, material properties and boundary conditions specified. The geometry is a half section of fin and tube, see Fig. 1, cut at lines of symmetry. On the insulated side of the tube, a constant heat flow equal to one percent of the bed side heat flow was used as boundary condition. This represents the radiation loss from the boiler wall

according to the DIN standard [13]. The heat flow on the bed side boundary of the tube was assumed to be constant, as a first approximation. A couple of repeated calculations, in which only this heat flow is changed, were carried out and the temperature difference between the two measurement positions (7 and 10 in Fig. 1) was evaluated and plotted against the heat flow. The relationship between temperature difference and heat flow was found to be linear with a proportionality constant C_3.

Since the actual heat flow is not constant around the tube, as discussed above, a correction factor F_i is defined in order to compensate the measured temperature difference for the spatial variation in heat flow. This gives the heat flux $\dot{q}_i$ for the ith measurement location as

$$\dot{q}_i = C_3 \frac{(T_{\text{fin}} - T_{\text{tube}})_i}{F_i}. \tag{6}$$

The variation in heat transfer around tube and fin depends on various parameters, such as geometry of the tube and the fin and the local distribution of particle concentration. Therefore, it is possible that the factor F_i varies from one position to another in the combustion chamber. However, until more information is available, it is assumed that the factor F_i is constant and the factor is denoted F. Its value is obtained from a comparison of the sum of heat power absorbed by the cold walls according to the fin-tube method and the total heat power $\dot{Q}_{cw}$ calculated from the heat balance over the combustion chamber

$$\sum_i (\dot{q}_i * A_i) = \dot{Q}_{cw}. \tag{7}$$

For a more detailed investigation of the variation of heat flow around the tube, ten thermocouples were mounted along the boundary of tube number 5 at height 7 m (Fig. 2) in all positions shown in Fig. 1.

RESULTS

For the operating conditions investigated, the average heat transfer coefficient at the cooling surfaces in the combustion chamber was 127 W m^{-2} K^{-1}, according to the heat balance.

The heat flow meters, when positioned at the center-line of a cold wall, recorded a heat transfer coefficient which decreased with elevation from 131 W m^{-2} K^{-1} at 2 m height to 93 W m^{-2} K^{-1} at 12.5 m, as shown in Fig. 6. In the horizontal direction, only a small variation in heat transfer could be detected by the heat flow meters at distances ± 0.5 m from the center-line, i.e. in the horizontal rows of holes shown in Fig. 2. Hence, this method underestimates the average value obtained from the heat balance with approximately 10% in this case. A possible reason for this is that the heat transfer rate varies around the tube with a higher value at the crest of the tube than at the fin where the meter was located.

Visual observations through holes in the CFB boiler

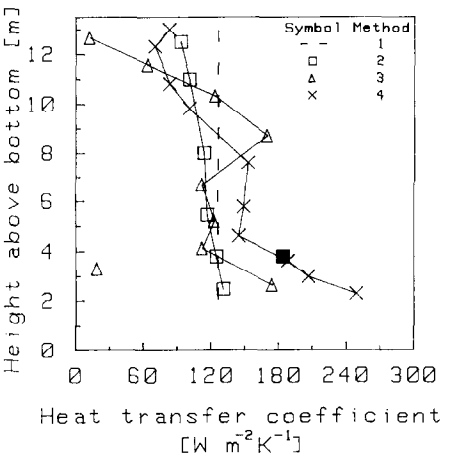

FIG. 6. Vertical distribution of heat transfer coefficient at boiler center-line. Results from different methods. Fin and tube temperatures are measured on tube number 4 (Fig. 2). The filled square shows the result from the heat flow meter with an obstacle located 0.5 m above it.

show that particles falling down at the walls tend to gather in the 'duct' formed by the tubes and the fin. As the particles fall along the wall they are cooled by the adjacent tubes and the lateral extension of the temperature boundary layer formed becomes larger at the fin than at the tube crest [11]. In addition, the cold particles shield the fin from the radiative heat flow from the bulk of the bed which further decreases the heat transfer at the fin. Thus, a higher concentration of particles, which normally gives a higher heat transfer coefficient, has an opposite effect in this case.

The tube temperatures (Method 3) along the center-line tubes give a heat transfer coefficient which is more dependent on height than that of the heat flow meters, see Fig. 6 in which results from tube number 4 (Fig. 2) are shown together with the other methods. At 2 m height the coefficient is about 35% higher than the average value in the combustion chamber. Up to 7 m height it is rather constant followed by a local maximum at 9 m. Eventually it decreases after 9 m and approaches zero due to boiling in the top of the tube where the method fails. The peak value at 9 m is found to be significant and more pronounced if the amount of primary air is increased. At 3 m height a very low value is recorded due to a very small temperature difference, less than one degree. The reason for this is not yet found, but it could be an effect of some irregularity in the suspension flow pattern caused by the upper edge of the refractory in the bottom zone.

An indication of the accuracy of this method is given in Fig. 7 where the heat transfer profiles from six tubes, numbers 2, 3, 4, 5, 7 and 8 (Fig. 2), are plotted. In the central part of the combustion chamber (2–9 m height) they differ around $\pm 30\%$. At higher elevations, the difference is small. The low value at 3 m height is found on three of the six tubes.

Data from the fin–tube method (Method 4) on the

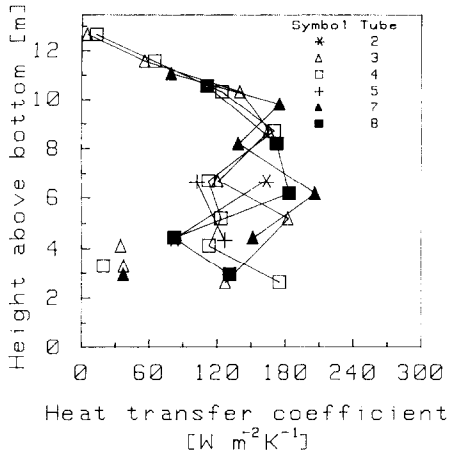

FIG. 7. Heat transfer profiles based on tube temperatures form six different tubes, number 2, 3, 4, 5, 7 and 8 in Fig. 2.

center-line tubes almost follow the same pattern as those from Method 3 but in the lower half of the combustion chamber the heat transfer coefficient is about 30% higher than that predicted by Method 3, as seen in Fig. 6. Moreover, the deviating values from the latter Method at 3 m height and in the top of the tubes, where boiling occurs, are avoided by the fin–tube method.

A certain variation of heat transfer is also found in the lateral direction across the walls. Figure 8 shows data from the horizontal rows 2, 5, 6, 7 and 9 numbered from the bottom in Fig. 2. Near the rear wall, on which the gas exit is located, the heat transfer is significantly lower than the cross-sectional average value at heights below the exit, i.e. below 9.5 m. A somewhat low value is also found close to the front wall. It is believed that the low heat transfer values are caused by the large down-flow of particles in the corners of the combustion chamber [14].

The overall heat transfer pattern in the combustion chamber seems to be rather symmetric, judging from

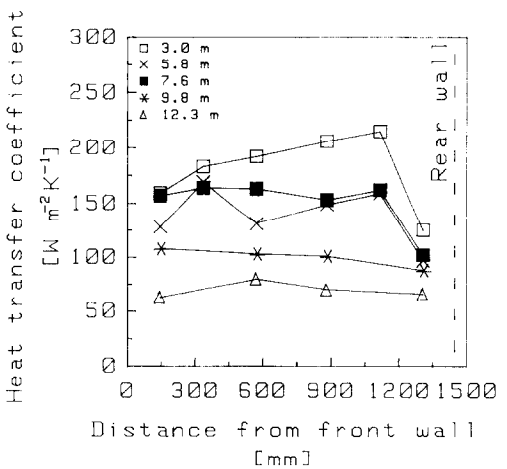

FIG. 8. Lateral distribution of heat transfer coefficient at different heights.

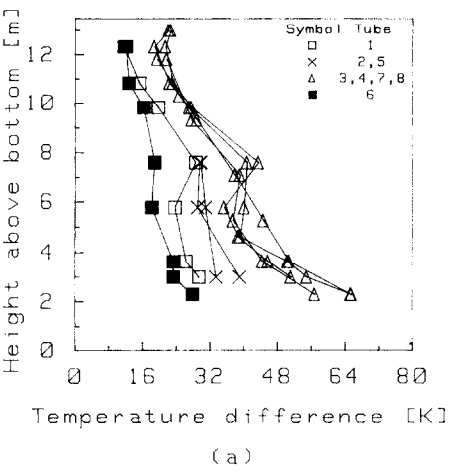

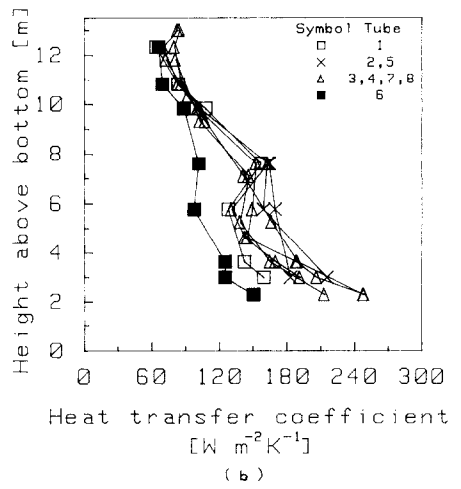

FIG. 9. Temperature differences (a) and corresponding heat transfer coefficients (b) for all instrumented tubes, see Fig. 2.

the small differences between the four center-line tubes on the opposite cold walls, numbers 3, 4, 7 and 8 in Fig. 2. The results differ less than $\pm 10\%$ as shown by the four curves with highest fin–tube temperature difference in Fig. 9a.

For the conversion of the temperature difference in Fig. 9a to a heat transfer coefficient in Fig. 9b, the difference in fin length is taken into account by means of the constant C_3 in equation (6), which has a lower value for the long fin than for the short one. The conversion brings together the profiles from short and long fins, except those measured in the corners, for reasons given above, which is a validation of the finite element analysis. The resulting scatter of the heat transfer profiles is considerably smaller than that obtained from Method 3.

In summary, the four methods compared, as represented in Fig. 6, determine the heat transfer coefficient with a scatter of $\pm 15\%$ in the central part (from 4 to 9 m) of the combustion chamber, where most of the heat is absorbed. In the lower part, only the methods based on wall temperature measurements

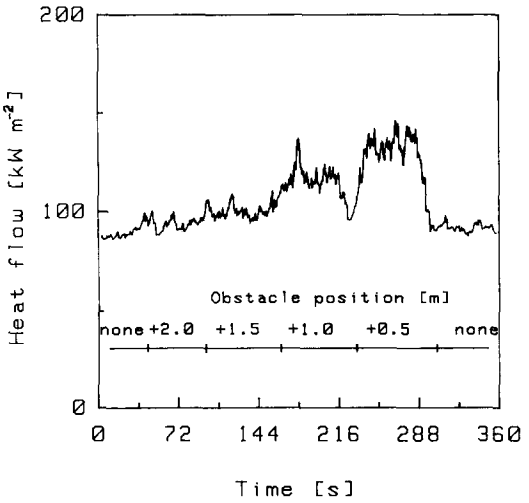

FIG. 10. Variation in heat flow measured by a heat flow meter at 3.8 m height with and without obstacle above the meter.

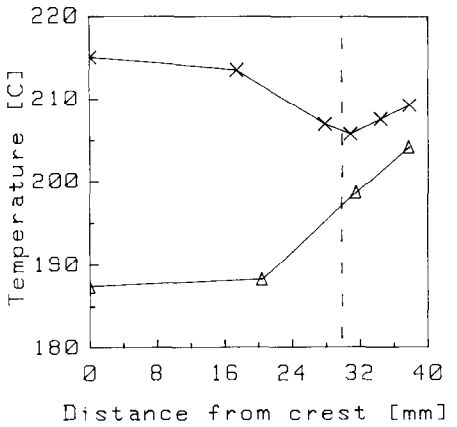

FIG. 11. Measured temperatures on bed side (X) and on insulated side (△) of the tube shown in Fig. 1. The dashed line indictes the outer tube diameter.

are able to detect the gradient in heat transfer and of these, the fin-tube method is the most accurate one.

Fin versus tube heat transfer

A possible reason why the heat flow meters do not detect the large heat transfer rates at heights below 4 m is that the flow of falling particles at the fins is larger than the flow at the tube and particularly large at low levels. To test this hypothesis a simple experiment was carried out. A heat flow meter was positioned at the center-line of the wall at a height of 3.8 m where the suspension density was about 25 kg m^{-3}. An obstacle in the form of a tube with the same diameter as the heat flow meter, i.e. 48 mm, was inserted 0.1 m into the combustion chamber, measured from the fin, at a height of 0.5 m right above the meter. This arrangement increased the heat transfer coefficient by 50%, measured by the heat flow meter at the fin, as shown in Fig. 10. It also more than doubled the amplitude of the signal. This change in character of the signal is similar to that recorded when the meter itself was inserted further into the combustion chamber, beyond the wall layer of falling particles and thus was exposed to the heat flow the bulk of the bed. Hence, the obstacle deflects the layer of falling particles from the fin for a certain distance downwards. This is interpreted as a verification of the hypothesis that the large down-flow of particles at the fin results in a low heat flow since the particles are cold and moreover they shield the fin from the radiative heat flow from the bulk of the bed. The heat flow increased by 50% above the normal heat transfer measurement is plotted with a dark symbol in Fig. 6. It happens to be almost the same as that obtained from the fin–tube method, which is sensitive both for the heat flow at the fin and at the tube.

The obstacle was also introduced at larger distances from the meter and still at a height of 2 m above the heat flow meter a small but significant influence on the signal could be observed, as seen in Fig. 10.

The experiment was repeated with the heat flow meter located at 10 m height and with the obstacle 1 m above it. At this level, where the suspension density was around 10 kg m^{-3}, as seen from Fig. 5, the obstacle did not affect the signal from the heat flow meter. This result was expected since there is no indication that the heat flow meter underestimates the actual heat flow at 10 m height, according to Fig. 6.

The temperatures measured on the tube instrumented with 10 thermocouples (tube number 5 at 7 m height) are given in Fig. 11. In the present case, the difference in temperature along the periphery of the tube and fin on the insulated side is 17°C which is smaller than those indicated in Fig. 9a for tube number 5 at heights around 7 m. This deviation is due to the geometry of the piece of tube with the ten thermocouples which is different from the normal tube geometry used in the present boiler. On the bed side, the temperature difference along the periphery is about 10°C. Although the temperature difference between the fin end and the tube crest on this side is only to 6°C, the character of the temperature variation at these two positions is rather different, as seen in Fig. 12. The amplitude at the tube crest is about three times that at the fin. Hence, the difference is similar to that observed with the heat flow meter when an obstacle was introduced right above it, as described previously and shown in Fig. 10.

In the finite element analysis it is possible to predict the temperatures on the insulated side of the tube with the boundary condition of an assumed constant heat flow on the bed side boundary. However, the hot side temperatures of the tube will not agree with the experimental values, as seen in Fig. 13. If the boundary is divided into parts with different heat flows it is possible to adjust the solution to the measured temperatures, which thus gives a quantitative estimation of the heat flow variation along the boundary. Already if the boundary is divided into three parts, as shown

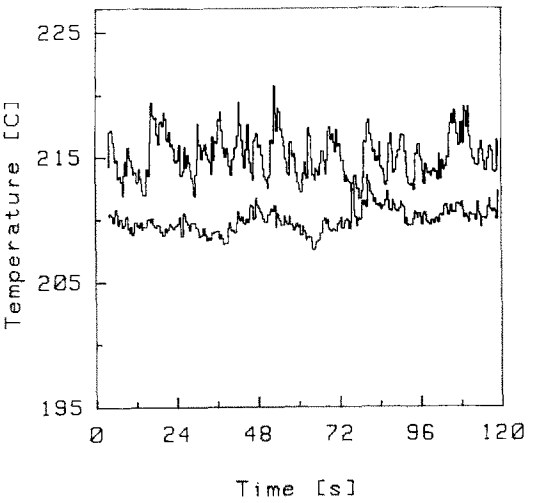

FIG. 12. Measured variation in temperature at the fin (lower curve) and at the tube crest (upper curve), i.e. at positions 6 and 1 in Fig. 1, at 7 m height.

in Fig. 14, it is possible to predict the temperatures within 1°C, see Fig. 13. The ratios of the heat flows applied on the tube crest, tube side and fin is 1.32 : 1.04 : 1 for the present case measured at a height of 7 m.

Heat transfer coefficient versus suspension density

The heat transfer coefficient including a radiation contribution, evaluated from wall temperatures, shows a strong dependence on the cross-sectional average suspension density in the whole range of suspension density investigated, 10–45 kg m^{-3}, whereas the heat flow meters only predict such a dependence up to 25 kg m^{-3}, for reasons discussed above. The fin–tube method gives a heat transfer coefficient, on the central part of the walls, varying from 80 to 250 W m^{-2} K^{-1} in the suspension density range 10–40 kg m^{-3}, as shown in Fig. 15.

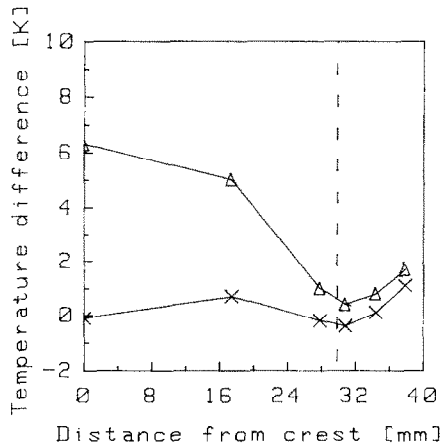

FIG. 13. Measured minus calculated temperatures on bed side of the tube in Fig. 1 with constant (△) and divided (X) heat flow boundary condition. The dashed line indicates the outer tube diameter.

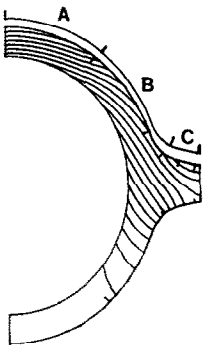

FIG. 14. Calculated temperature field, represented by isotherms, at divided (A, B and C) heat flow boundary condition on bed side of the tube.

DISCUSSION

Methods

In a conventional CFB steam boiler, two of the methods treated are not suitable; local heat flow meters and local water temperature. The fin–tube temperature method, however, can be used, and if it is compared with the heat balance over the combustion chamber, the correction factor F_i in equation (6) can be estimated and the accuracy of the method is increased. The calculation of the heat balance on a steam boiler, is more complex than on a hot-water boiler, such as the present one. Therefore, the method may be less accurate for a steam boiler. The accuracy of the temperature field calculation in the fin–tube method depends on how well the geometry of the tube and fin is known, particularly that of the fin–tube junction. In the 'American type', mentioned above, the junction may be irregular and less well-defined due to the two welds. The tube temperature method may be used in laboratory scale equipment [6]. However, if the cooling medium is water, rather long tubes are required to reach a sufficient temperature difference for a high accuracy of the heat transfer coefficient

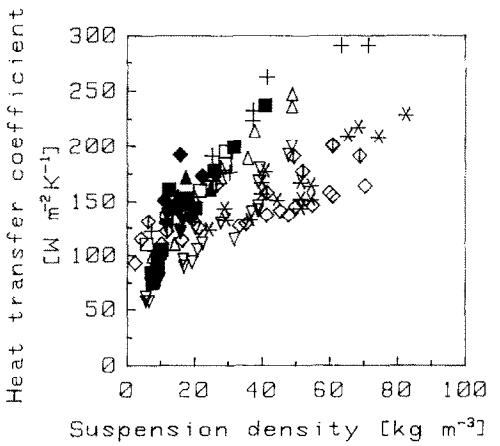

FIG. 15. Heat transfer coefficient vs cross-sectional average suspension density. High temperature data from literature and present investigation, see Table 2.

Table 2. Parameter description for high temperature heat transfer data in Fig. 15

Symbol	Reference	Particle diameter (μm)	Bed temperature (°C)	Bed width (m)	Length of heat transfer surface (m)
*	Kobro [15]	250	850	0.2	0.1
+	Kobro [15]	170	850	0.2	0.1
▼	Andersson [3]	240	750	0.7	0.01
▲	Andersson [3]	240	800	0.7	0.01
◆	Andersson [3]	240	850	0.7	0.01
□	Basu [16]	296	885	0.202	0.1
◈	Wu [17]	241	880	0.152	1.53
◇	Wu [17]	222	870	0.152	1.53
△	Basu [1]	296	895	0.202	0.1
▽	Basu [1]	296	815	0.202	0.1
■	This study	312	850	1.7	1 to 10

calculated. Hence, local values of heat transfer are difficult to obtain by this method.

It is shown above that the particles falling down near the fin remain at the wall for lengths which are in the order of meters, i.e. for times in the order of seconds, which by far exceed the thermal time constant of 300 μm diameter particles [15]. This means that at long membrane walls, such as in a boiler, the particles close to the fin can be assumed to be at equilibrium temperature and the length over which the heat flow is estimated becomes less important. Moreover, the heat flow meter used is small enough not to significantly influence the temperature of the particles as they pass the heat flow meter. Hence, the meter will measure a value representative for the fin at the actual location.

Heat transfer coefficient versus suspension density

The heat transfer coefficient is related to the cross-sectional average suspension density, although other factors also may have a certain influence such as the geometry of the bed and the wall surface, particle size distribution, temperature, length of meter etc.

High temperature CFB heat transfer data found in literature and the present values from Method 4 are compared in Fig. 15 as a function of suspension density. The range of density covered is wide enough to include the densities occurring in commercial CFBBs. The figure gives an overall impression of a certain scatter which is not surprising given the large differences in the conditions at which the various sets of data were obtained, e.g. bed diameters in the range 0.2–1.7 m and length of heat transfer surfaces varying from 0.01 m to several meters. In spite of the differences in experimental conditions, a simple square root relationship, equation (8), is able to predict most of the experimental high temperature data within $\pm 30\%$ if the constant C_4 is put to 30,

$$\alpha = C_4\sqrt{\rho_b}. \tag{8}$$

The data on membrane wall heat transfer from Wu *et al.* [17] differ from the other sets of data since they are linearly dependent on the suspension density.

It should be noted that equation (8) obviously is not valid at low suspension densities.

In the present investigation only one test run of the boiler has been studied since the main aim is to evaluate the experimental methodology, but the case and the data are of significance as an example of heat transfer during normal operating conditions of a CFBB. The influence from various design and operational parameters on the heat transfer in the present boiler is treated elsewhere [19].

CONCLUSIONS

Four different methods have been used to estimate the coefficient for heat transfer between the bed and the cold membrane walls in a hot-water CFBB during normal operating conditions. The results from the various methods agree within $\pm 15\%$ in the central part of the combustion chamber.

Some of the methods are found to be less accurate at certain conditions. For example, the heat flow meters underestimated the heat transfer since they measured at the fin where a large down-flow of cold particles decreased the heat flow from the bulk of the bed to the wall. The fin–tube method, on the other hand, seems to be a reliable and easy to use method to obtain local heat transfer results in hot-water as well as steam boilers, particularly if the average heat absorption of the combustion chamber can be evaluated by a heat balance.

A significant variation in heat flow was detected around the fin–tube periphery. A finite element analysis of the temperature field in the tube indicated a 30% higher heat flow at the crest of the tube than at the fin at the location of measurement. The fin–tube method, thus, gives an average value around tube and fin.

In the vertical direction, the heat transfer coefficient was almost constant and around 130 W m^{-2} K^{-1} in the case studied. Close to the corners of the com-

bustion chamber the heat transfer was smaller than in the central part.

Acknowledgements—The authors are grateful to ABB Corporate Research Dept KEB, Västerås, Sweden for the possibility of using the finite element program Ace and to the Swedish National Energy Administration for financial support.

REFERENCES

1. P. Basu, Heat transfer in high temperature fast fluidized beds, *Chem. Eng. Sci.* **45,** 3123–3136 (1990).
2. R. Pich, Die theoretische Ermittlung der Temperaturverteilung in den Flossen von Walther-Flossenwänden, *Energie* **15,** 12–16 (1963).
3. B.-Å. Andersson, F. Johnsson and B. Leckner, Heat flow measurements in fluidized bed boilers. In *Proc. of the 9th Int. Conf. on Fluidized Bed Combustion*, Vol. 1, pp. 592–598, ASME Book No. 10232A, New York (1987).
4. S. E. Gustafson, E. Karawacki and A. Chohan, Thermal transport studies of electrically conducting materials using the transient hot-strip technique, *J. Phys. D: Appl. Phys.* **19,** 727–735 (1986).
5. B.-Å. Andersson, F. Johnsson and B. Leckner, Use of a conductivity heat flow meter in fluidised bed boilers, *Trans. Inst. Measure. Control* **11,** 108–112 (1989).
6. R. L. Wu, C. J. Lim, J. Chaouki and J. R. Grace, Heat transfer from a circulating fluidized bed to membrane waterwall surfaces, *A.I.Ch.E. Jl* **33,** 1888–1893 (1987).
7. Ya. S. Žoludov and E. I. Konoplev, Calculation of temperature conditions in finned tubes for membrane walls, *Teploenergetika* **12,** 71–74 (1965).
8. D. R. Raymond and J. W. Rausher, Heat transfer determination in boiler waterwall tubes using fin temperature measurements, *Tappi Journal* **67,** 76–79 (1984).
9. L. Jestin, C. Chabert, G. Flamant and P. Meyer, In-situ measurement of particle concentration, temperature distribution and heat flux in the vicinity of a wall in a CFB. In *Circulating Fluidized Bed Technology—III* (Edited by P. Basu, M. Horio and M. Hasatani), pp. 247–252. Pergamon Press, Oxford (1991).
10. B. D. Bowen, M. Fournier and J. R. Grace, Heat transfer in membrane waterwalls, *Int. J. Heat Mass Transfer* **34,** 1043–1057 (1991).
11. B. Leckner, M. R. Golriz, W. Zhang, B.-Å. Andersson and F. Johnsson, Boundary layers-first measurements in the 12 MW CFB research plant at Chalmers University. In *Proc. of the 11th Int. Conf. on Fluidized Bed Combustion*, Vol. 2, pp. 771–776, ASME, ISBN No. 0-7918-0619-7, New York (1991).
12. Finite Element Program Ace version 1.6, ABB Corporate Research Dept. KEB, S-721 78 Västerås, Sweden (1991).
13. Deutsche Industrie Norm No. 1942, VDI-Rules for Steam Generators, Deutsches Institut für Normung, Berlin (1979).
14. B. Leckner and B.-Å. Andersson, Characteristic features of heat transfer in circulating fluidized bed boilers. *Powder Technol.* **70,** 303–314 (1992).
15. H. Kobro and C. Brereton, Control and fuel flexibility of circulating fluidised bed. In *Circulating Fluidized Bed Technology* (Edited by P. Basu), pp. 263–272. Pergamon Press, Toronto (1986).
16. P. Basu and F. Konuche, Radiative heat transfer from a fast fluidized bed combustor. In *Circulating Fluidized Bed Technology—II* (Edited by P. Basu and J. F. Large), pp. 245–253. Pergamon Press, Oxford (1988).
17. R. L. Wu, J. R. Grace, C. J. Lim and C. M. H. Brereton, Suspension-to-surface heat transfer in a circulating-fluidized-bed combustor, *A.I.Ch.E. Jl* **35,** 1685–1691 (1989).
18. L. R. Glicksman, Circulating fluidized bed heat transfer. In *Circulating Fluidized Bed Technology—II* (Edited by P. Basu and J. F. Large), pp. 13–29. Pergamon Press, Oxford (1988).
19. B.-Å. Andersson and B. Leckner, Bed-to-wall heat transfer in circulating fluidized bed boilers, The Second Minsk International Heat and Mass Transfer Forum, Luikov Heat and Mass Transfer Institute, Minsk (1992).